

Simulating Decadal Sedimentation in the Upper Indus Basin and Tarbela Reservoir Using SWAT Model

Nimra Arshad ², Nausheen Mazhar ¹, Paul Passy ²

¹ Department of Geography, Lahore College for Women University, Pakistan

² Department of Geography (UMR PRODIG), Université Paris-Cité (University of Paris), France

* Correspondence: nausheen.mazhar@lcwu.edu.pk

Abstract

Tarbela Reservoir, one of Pakistan's key irrigation and hydropower sources, has experienced diminishing live storage due to high sediment generation from the Upper Indus Basin (UIB), over the past three decades. This study monitors sedimentation trends from 1994 to 2023 using Satellite data from USGS STRM, ERA5-Land Climate Reanalysis, FAO's Digital Soil Map of the World, and Global Land Cover dataset. Ground data came from the Surface Water Hydrology Project and Tarbela Dam Project Library. Using ArcSWAT, a 30-year model was developed for a 102,028 km² area, with 64 HRUs and 26 subbasins to assess spatial heterogeneity. Sensitivity analysis, calibration, and validation were performed using SWAT-CUP and SUFI-2 algorithm showing excellent model performance with 22 parameters. The model achieved R² of 0.89, NSE of 0.84 during calibration, and R² of 0.81, NSE of 0.68 during validation. Model simulations for the Upper Indus Basin at Besham Qila show 78% of precipitation contributes to stream flow, with 61% as surface runoff. July presents peak rainfall, sediment yield, and water flow. Annual surface runoff averages 505.35 mm, with upland sediment yields from 5,772.90 to 2,086.09 Mg/ha. Significant in stream sediment deposition (-2,082.52 Mg/ha) heightens flood risks. Decadal sediment yield decreased from 5.9–385.3 tons/ha to 2.7–370.6 tons/ha. Reforestation, terracing, check dams, and sustainable land use practices are recommended to control sediment generation and deposition in Tarbela reservoir. Continuous monitoring and stakeholder engagement are essential to maintain reservoir storage capacity and hydropower efficiency.

Keywords: SWAT; SWAT-Cup; Tarbela Dam; Sedimentation; Upper Indus Basin

1. Introduction

Reservoir serve as open air storage for water withholding sufficient quantity to be drawn off for use. Reservoirs are a critical component of many water supply systems around the world” (Britannica, 2020). Reservoirs constructed normally across the river (Jorgensen, Löffler, Rast, & Straskraba, 2005) and is typically located at the end of a catchment, collecting inflows from various major rivers (Merina, Sashikkumar, Rizvana, & Adlin, 2016). Large dam construction peaked in the 1960s and 1970s, and there are now nearly 60,000 such dams worldwide (ICOLD, 2020). Reservoirs and dams are two of the most common engineering management approaches serve various purposes such as with droughts, floods, and water scarcity (Gaupp, Hall, & Dadson, 2015). By releasing water stored during the wet season, reservoirs can potentially cover or reduce water deficits during the dry and high-demand seasons (Kellner, 2021). Since the construction of dams have they been used to store water for agricultural, industrial, and household purposes (Merina et al., 2016).

Hydroelectric dams also serve as an alternative to nonrenewable energy resources, which account for the vast majority of the world's energy (UCSUSA, 2013). Dams can harvest gravitational potential energy and use it to generate electricity at low rates. Hydroelectric dams provide 19% of the world's electricity supply. 30 to 40 percent of the 271 million hectares that are irrigated worldwide rely on irrigation dams (WWF, 2013). Reservoirs can help prevent downstream flooding by holding and regulating flow during major flood events (Goel & Jain, 1996; Lindström & Grani, 2012). Reservoirs can also be used to balance flow during different weather conditions, such as decreasing flow during heavy rainfall and increasing flow during droughts (Mukherjee, Veer, Tyagi, & Sharma, 2007; X. Wang, Shao, & Li, 2003). The filling of reservoirs of large dams has been known to cause seismic activity due to the physical change incurred in the area where the reservoir was filled, as well as the dam's activity (Houquin, 2010).

The threat of sedimentation is threatening the world's reservoirs however existing reservoirs around the world are under threat from what Silvio and Hotchkiss (1995) refer to as 'insidia solida'. According to Merina et al. (2016) Natural processes are responsible for reservoir sedimentation. Rivers and streams within a catchment area are constantly subjected to sediment from runoff, precipitation, snowmelt, and channel erosion.

The gradual filling of reservoirs with sediment is a major cause of the decrease in performance. Dams obstruct the natural movement of sand, soil, and rocks along rivers, preventing them from reaching their destinations (Annandale, Morris, & Karki, 2016). Because of sediment accumulation and deposition, reservoir sedimentation reduces functional storage capacity (Foteh et al., 2018; Goel, Jain, & Agarwal, 2002; Vemu & Udayabhaskar, 2010). Regrettably, the accumulation of sediment deposits causes a plenty of reservoirs to cease functioning (Ijam & Al-Mahamid, 2012; Merina et al., 2016). The buildup of sediment in the reservoir leads to a decrease in its capacity, disrupts its operational efficiency, and could potentially accelerate the wear and tear of the hydraulic infrastructure situated on the barrage. This, in turn, reduces the effectiveness of its intended functions and may lead to increased maintenance expenses (Ayele et al., 2021). On the other hand, human actions and interventions in the upstream watershed exacerbate accelerated reservoir sedimentation. While soil erosion is a result of geomorphological processes, it is primarily driven by human activities. Rapid population growth, deforestation, inappropriate land cultivation, and unchecked overgrazing have all accelerated soil erosion, particularly in developing countries around the world (Abebe & Sewnet, 2014; Merina et al., 2016; Tamene, Park, Dikau, & Vlek, 2006). Perera, Williams, and Smakhtin (2023) estimate that sedimentation in 47,403 big dams across 150 nations might result in the loss of nearly 26% of water storage capacity by 2050. With some regions having already lost 13-19%. Countries like Seychelles, Japan, Ireland, Panama, and the UK could lose the most (35-50%), while Bhutan, Cambodia, Ethiopia, Guinea, and Niger might lose the least (under 15%). This reduction in water storage will impact things like irrigation, farming, power, and water supply. Previous research on the Tarbela Reservoir has mostly focused on silt deposition inside the reservoir or sediment yield prediction. However, detailed evaluations of sediment output over the Tarbela watershed region are rare. Reservoir sedimentation is a common problem that, although hard to totally eliminate, may be efficiently controlled by upstream watershed improvements. Understanding the dynamics of sediment output from upstream catchments and reservoir sedimentation is critical for mitigation measures. In this work, the SWAT model is being used to examine the sediment yield behavior of the Tarbela Reservoir catchment.

2. Study Area Description and Data Used

2.1. Study Area

Tarbela Dam is one of the largest earth-fill dams in the world (Moiseev, 2000; Nayab & Faisal, 2018). This dam is built on the Indus River and is situated in Khyber Pakhtunkhwa province of Pakistan and is approximately 130 kilometers in the North of Islamabad. The construction of the dam started in 1970 and was completed in 1974 by the

Pakistan's Water and Power Development Authority (WAPDA). The Tarbela Dam is named after the town of Tarbela, which is located in the districts of Haripur and Swabi. It is located at 34°05'23" N-72°41'55" E (Mazhar et al., 2021). The main dam is an earth core rock fill dam with a length of 2743 metres and a height of 148 metres (Roca, 2012). The length of the Indus River upstream of Tarbela Dam is approximately 1100 km, with a catchment area of approximately 169,645 km². The majority of the upper Indus Basin area is made up of snow-covered high mountains, while the catchment monsoon area is only 10,360 km² just above Tarbela (Aslam, 1992). It is also the second largest dam in the world in terms of reservoir capacity, which is 11.62 million acre-feet (Nayab & Faisal, 2018).

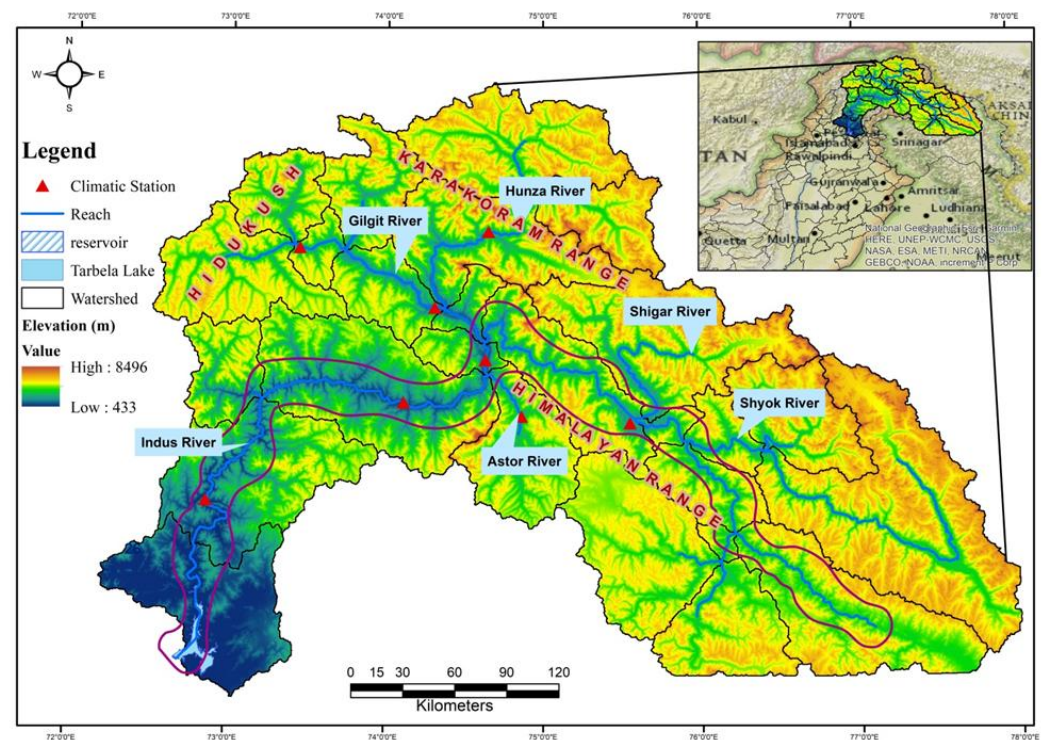


Figure 1. Study Area (Tarbela dam with its watershed delineate by SWAT model.)

3. Material & Methods

3.1. Data Used for Sediment Yield Modeling

This study's data gathering technique guarantees that complete and reliable inputs are obtained for the analysis and prediction of sedimentation in the Tarbela Reservoir. Secondary and ground-observed data were used to improve the validity and reliability of the results. The key input data for the SWAT model were obtained from global and national sources. Satellite data included a 30-meter resolution Digital Elevation Model (DEM) from USGS SRTM, precipitation and temperature data from ERA5-Land Daily Aggregated (ECMWF Climate Reanalysis via GEE), soil data from the FAO's Digital Soil Map of the World (DSMW), and land cover information from the Global Land Cover dataset at Level 4 for 2009. Ground-observed data from the Tarbela Dam Project, released by the Water and Power Development Authority (WAPDA), comprised discharge data from Besham Qila between 1994 and 2023. Collectively, this diversified information allows for a thorough investigation of sediment dynamics in the reservoir during the last 30 years, confirming the correctness of sedimentation process estimates. The overall methodology adapted in the present study is shown in Figure 2.

4. Methodology

The study utilized SWAT model to analyze sedimentation this work used numerous datasets to simulate sediment output and reservoir sedimentation in the Tarbela Reservoir. DEM data was mosaicked and projected to WGS 1984 UTM Zone 43N for hydrological modeling, which allowed for flow accumulation, watershed delineation, and slope analysis. Streamflow data from Besham Qila (1994-2023) was converted to SWAT-compatible formats for calibration and validation. Climatic data from ERA5-Land (daily precipitation and temperatures) were processed and structured for SWAT input, allowing the Custom Weather Generator to be activated. Soil data from the FAO's DSMW was rasterized, cropped, and referenced to fit the research region, and a lookup table of soil properties aided SWAT compatibility. Land use data from the Global Land Cover dataset (2009) were spatially clipped and reclassified to SWAT land use codes, which linked surface processes such as runoff and sediment generation to land cover categories. SWAT simulations were calibrated and validated using SWAT-CUP and the SUFI-2 methodology. Sensitivity analysis was carried out in SUFI-2 utilizing a global sensitivity technique that ranks parameters according to their p-value and t-statistic. Calibration and validation involved comparing real and simulated streamflow data using performance indicators like Nash–Sutcliffe Efficiency (NSE), Percent Bias (PBIAS), and Coefficient of Determination (R^2). The parameter ranges were adjusted iteratively to improve model performance within the 95% prediction uncertainty (95PPU) regions. This comprehensive technique enabled accurate simulation of sedimentation dynamics and watershed processes.

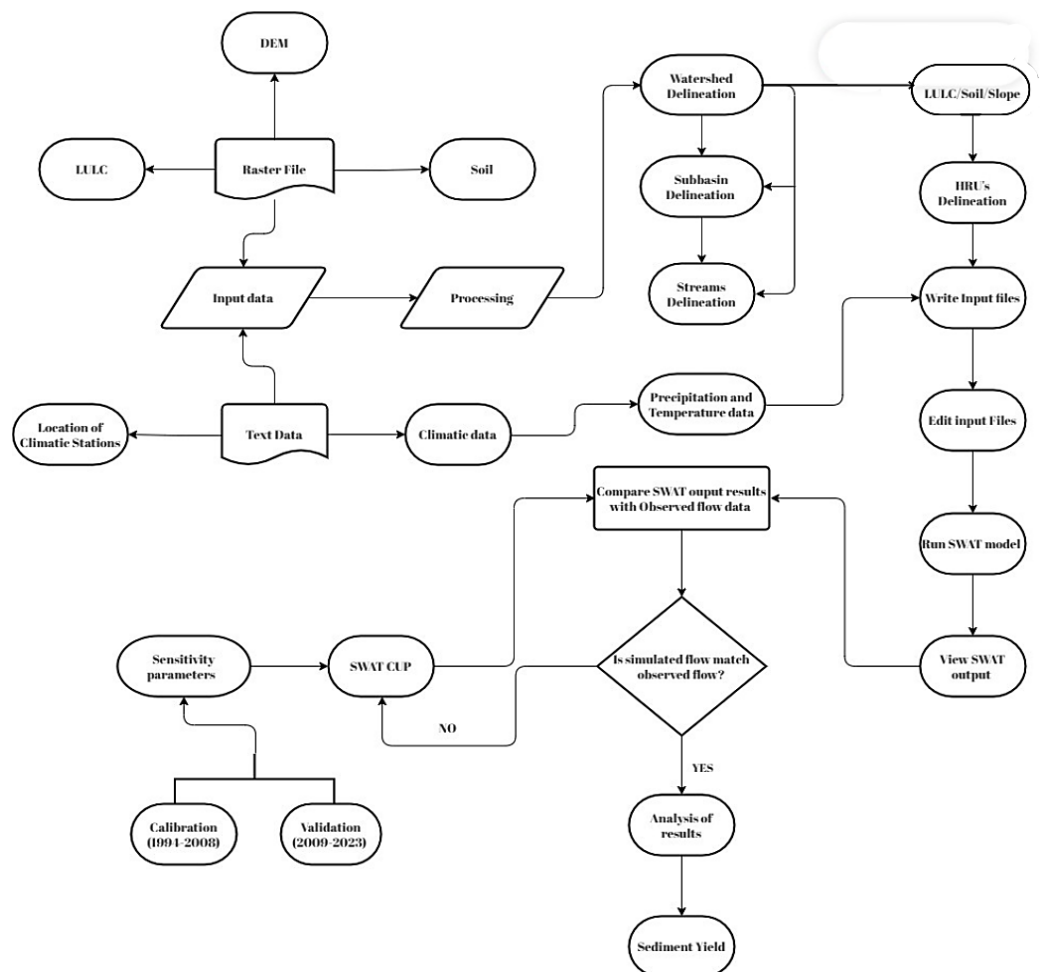


Figure 2. Methodology for Hydrological Modeling and Sediment Yield Analysis using ArcSWAT and SWAT-CUP.

5. Results & Discussion

The SWAT model calculated yearly sediment output from the reservoir catchment during a 30-year period (1994-2023). 26 subbasins were created within the study region as a result of the watershed being delineated using USGS SRTM DEM with a 30-meter resolution. The thorough elevation data provided by this high-resolution DEM is essential for accurate watershed delineation. The DEM has a large range of elevation, ranging from the lowest point of 433 meters to the highest point of 8496 meters with the average height of 3948.40 meters, and the standard deviation of 1227.42 meters. Watershed delineation provides the flow paths, drainage network, hydrological system and the overall geographical area and sub areas. Realistic modeling of runoff, deposition, erosion, and water balance is essential for the management and planning of the water resources of the region. In the HRU definitions, the features that include at least 25% of a subbasin are considered, with a threshold of 25% applied to LULC, soil type, and slope. This approach ensures that the model incorporates the most crucial land cover and soil classes hence enhancing the model's accuracy. The gradient was classified as 0-5%, 5-10%, 10-15%, 15-30%, and 30-9999%, thus providing a complete representation of the topographical variation. By adhering to the thresholds and ranges of LULC, soil, and slope data, A total of 64 Hydrologic Response Units (HRUs) were defined using unique combinations of land use, soil type, and slope class. This extensive categorization enables the model to take into account a greater number of hydrological variables and interactions within the watershed leading to more precise approximations of runoff, erosion, and other hydrological processes.

Table 1. Major Land Use, Soil and Slope classes in study area watershed as per SWAT model domain.

	Types	Area[acres]	%Water Area
LANDUSE			
	Agricultural-Land-Generic (AGRL)	1747637.33	6.93
	Hay (HAY)	625826.73	2.48
	Forest-Deciduous (FRSD)	403738.14	1.6
	Forest-Mixed (FRST)	130510.62	0.52
	Pasture (PAST)	208344.90	0.83
	Range-Grasses (RNGE)	11365171.23	45.08
	Wetlands-Forested (WETF)	6103.12	0.02
	Residential (URBN)	2997.20	0.01
	Barren (BARR)	5337471.65	21.17
	Water (WATR)	5383920.64	21.35
SOILS			
	Ao72-2b (Sandy Loam)	1133038.49	4.49
	Be72-2a (Loam)	1764704.35	7
	Be72-2c (Loam)	962150.94	3.82
	Be72-3c (Loam)	43048.01	0.17
	Be73-2c (Clay)	1387739.21	5.5
	Be78-2c (Loam)	585542.98	2.32
	GLACIER	5011226.13	19.88
	I-B-U (Loam)	6870800.72	27.25
	I-B-U-2c (Loam)	4787242.94	18.99
	I-X-2c (Loam)	52769.5286	0.21
	I-Y-2c (Loam)	2558840.72	10.15
	Rc40-2b (Loam)	54617.54	0.22

SLOPE			
	0-5	791061.51	3.14
	5-10	963020.60	3.82
	10-15	1091854.03	4.33
	15-30	4264672.41	16.92
	30-9999	18101113.04	71.8

5.1. SWAT Model Calibration and Validation

Calibration of SWAT model parameters is required to ensure that model outputs, such as streamflow and sediment yield, closely match actual data. This stage is critical since each watershed has distinct features determined by elements such as soil properties, land use patterns, and climate conditions. The default parameter choices may not effectively represent these local variables, therefore calibration helps to adjust the model to the unique watershed for more trustworthy and realistic simulation results. Calibration of the model also helps to capture specific characteristics of the watershed and enhance the simulation results (Ming et al., 2022). Validation checks the calibrated model against data that have not been used in calibration process. This technique helps the model to make reliable predictions of watershed behavior in a variety of situations, including changes in land use and climate (Paudel et al., 2021). In this study, 22 SWAT parameters influencing snow, glacier melt runoff, groundwater recharge, and evapotranspiration were calibrated (modified) to align simulated results closely with observed data as given in Table 1 This was achieved through sensitivity analysis, supplemented by a review of relevant literature on snow and glaciated mountainous regions (Ahl, Woods, & Zuuring, 2008; Malik, Dar, & Jain, 2022; Pradhanang et al., 2011; Rahman et al., 2013).

Table 2. Statistical assessment of simulated and observed model results.

Coefficients	Calibration Period (1994-2008)		Validation Period (2009-2023)	
	Observed	Simulated	Observed	Simulated
Mean		2855.13 cms		2890.02 cms
r-factor		0.92		0.71
p-factor		0.68		0.69
R ²	2426.66 cms	0.89	2447.44 cms	0.81
NSE		0.84		0.68
P _{BIAS}		-17.7		-18.1
RSR		0.39		0.57

The average flow rate observed during the calibration period was 2426. 66 (cms) as compared to the simulated mean flow which was found to be 2855. 13 (cms), which is slightly overestimated by the model. According to widely recognized hydrologic model evaluation standards as given in Table 3 The model showed "Very good" with a R² value of 0.89, showing a strong correlation between observed and simulated data. The NSE score of 0.84 implies that model simulations were very consistent with observed data, supporting the "Very good" performance grade. The PBIAS of -17.7% is somewhat exaggerated but still within the less than twenty percent range, suggesting "Very good." The RSR value of 0.39 confirms the model's high fit, indicating that mistakes are low relative to data variability. The p-factor and r-factor values of 0.68 and 0.92 show that most observed data falls inside the model's uncertainty boundaries, suggesting low prediction uncertainty. During the validation period, the observed mean flow was 2447.44 cms, while the

simulated mean flow was 2890.02 cms, indicating that the model overestimated the flow slightly. The R^2 score of 0.81 indicates a substantial connection between observed and simulated values, retaining the "Very good" classification. The NSE value of 0.68, although significantly lower than during the calibration period, suggests that the model's performance is still good, verging on excellent. The PBIAS of -18.1% remains slightly overestimated, but it falls within the acceptable "Very good" range. The RSR score rose to 0.57, indicating that errors relative to observed data variability have somewhat risen, but the model fit remains good. During validation, the p-factor and r-factor values were 0.69 and 0.71, respectively, showing that the model continues to capture the majority of the observed data within its uncertainty bounds, although with somewhat higher prediction uncertainty than during calibration. Overall, it was found that the SWAT model performed reasonably well for the Besham Qila River for the calibration and validation period. The comparison of R^2 , NSE, PBIAS, and RSR values shows that the calibration of river flow simulation in the model is acceptable.

Table 3. SWAT model evaluation criteria based on (Tanteliniaina et al., 2021).

Variable	Value	Performance Rating
NSE (Nash-Sutcliffe Efficiency)	>0.65	Very good
NSE	0.54 to 0.65	Good
NSE	<0.5	Satisfactory
PBIAS (Percent Bias)	$<20\%$	Very good
PBIAS	20% to 40%	Good
PBIAS	$>40\%$	Unsatisfactory
R^2 (Coefficient of Determination)	$R^2 > 0.7$	Very good
R^2	$0.5 < R^2 < 0.7$	Good
R^2	$R^2 < 0.5$	Satisfactory

Table 4. Water Balance ratio of the watershed.

No.	Variables	Value
1	Streamflow/Precipitation	0.78
2	Baseflow/Total Flow	0.39
3	Surface Runoff/Total Flow	0.61
4	Percolation/Precipitation	0.16
5	Deep Recharge/Precipitation	0.01
6	ET/Precipitation	0.05

The SWAT Check analysis identifies water distribution within the boundaries of the watershed and offers crucial ratios for watershed assessment. These ratios are employed in the management of land use, water resources, erosion, floods, and sustainable groundwater management in watersheds. The importance of contemporary management approaches is also apparent. These ratios should be understood and enhanced by the watershed managers in order to sustain the water resources and the ecosystem. Table 4 presents the basic parameters of the water balance of the watershed for the assessment of water flow. According to this ratio, 78% of the watershed precipitation contributes to the streamflow. The surface runoff and the base flow from the river systems indicate that the area receives a lot of rainfall. Base flow, the part of the groundwater that contributes to streamflow, is 39%. Streamflow during the dry season depends on subterranean water. Surface runoff forms 61% of the total stream flow while runoff coefficient is zero. Direct runoff contribution to the streams and rivers during precipitation. It is estimated that as much as 16 percent of the rain seeps into the ground to recharge the groundwater. Percolation

helps in maintaining stable water tables and base flow. The precipitation refills the aquifers to one percent only. In watersheds with shallow aquifers, the deep aquifers are not recharged to a great extent. Precipitation loss through evapotranspiration is at 5%. This is the amount of water that drains through the soil to evaporate and transpire and is sent back to the atmosphere by evaporation and plant transpiration.

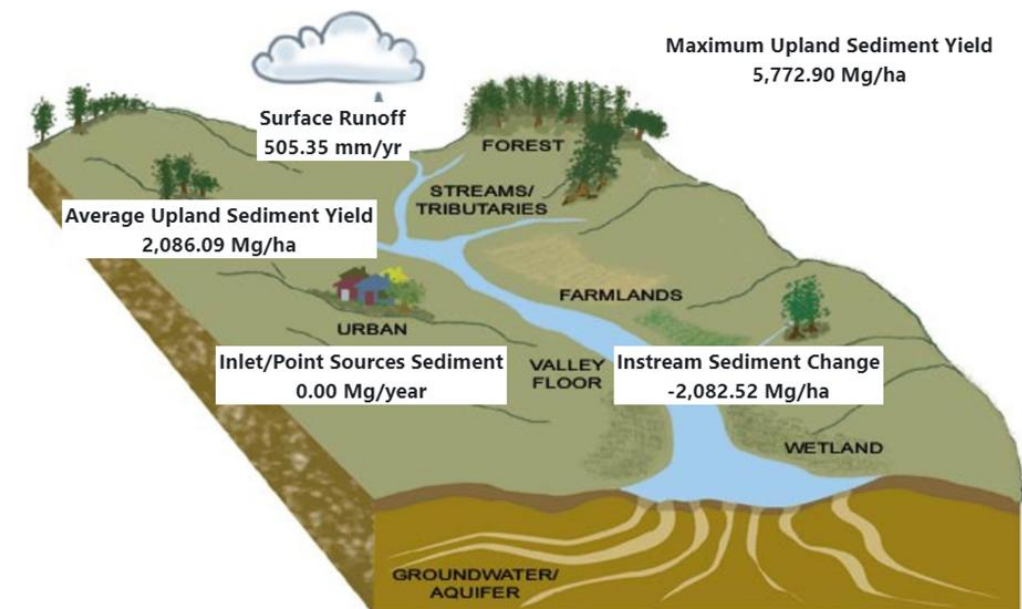


Figure 3. Sediment Dynamics in Watershed: 30-Year SWAT Model Output (1994-2023).

Figure 3 demonstrate upland sediment yields range from a maximum of 5,772.90 Mg/ha to an average of 2,086.09 Mg/ha. These numbers show a significant loss of sediment from the landscape, which is probably caused by a combination of the region's steep slopes, soil composition, land use, and vegetation cover. The high maximum yield raises the possibility that some parts of the watershed—possibly deforested or poorly managed agricultural lands—are making a disproportionate amount of sediment (Gashaw et al., 2022). The watershed shows an instream sediment change of -2,082.52 Mg/ha, which suggests that rivers and streams are serving as sinks rather than sources of material. This study demonstrates that sediment fills the stream channels, thus decreasing the water-carrying capacity and enhancing the flood risks. The elevated highest sediment yield emphasizes the importance of the movement of sediment in watershed hydrology, with major implications for streams water quality and dam sedimentation.

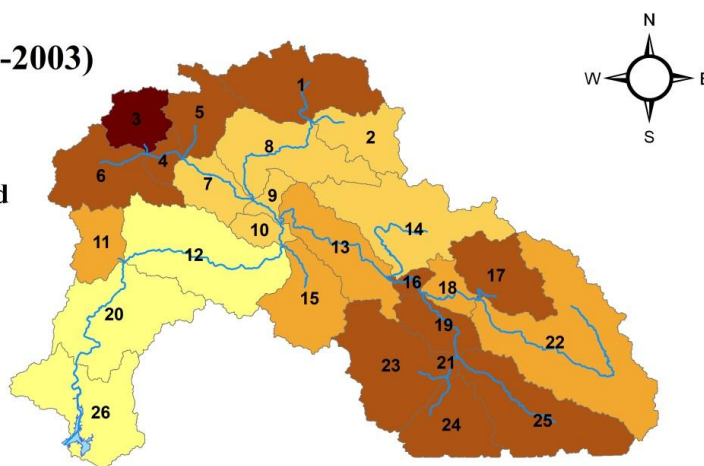
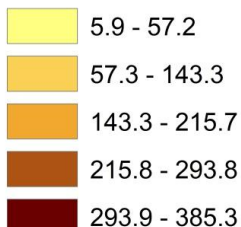
5.2. Spatial Trend analysis of sediment yield over Subbasins for Three Decades

The outflow of Upper Indus Basin UIB Watershed is Tarbela reservoir; subbasin sediment output changes are particularly notable. As reservoir is located within the subbasin 26 so all the sediment from the upper Indus Basin outflow from the Tarbela reservoir some particles remain suspended in the water and some are being deposited creating a under-water Delta so that's why sediment delivery is crucial to its lifespan and efficacy. The reservoir's location in Subbasin 26 emphasizes the vital role of sediment supply for assessing its longevity and operational effectiveness. Sediment deposition can reduce reservoir capacity for storage, decrease the efficiency of operation, and eventually shorten the reservoir's usable lifespan. The SWAT model can be used to simulate sediment yield and quantify sediment transport from particular subbasins, as well as examine how such contributions have changed over a period of thirty years.

(a)Decade_1 (1994-2003)

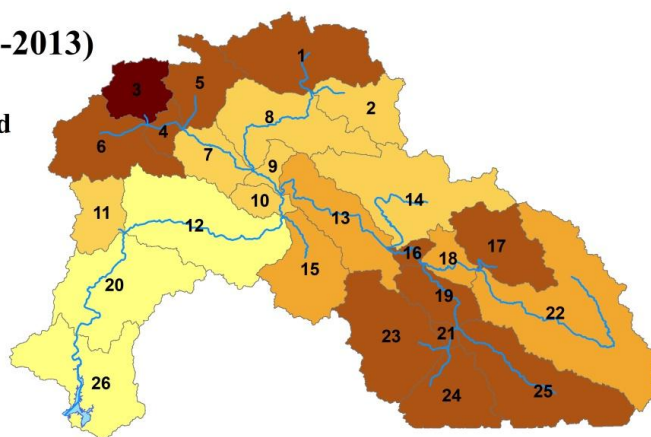
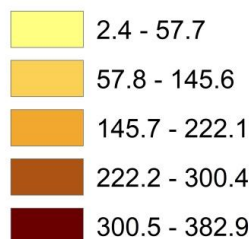
Legend

— Reach
Average Sediment Yield
(tons/ha/decade)



(b)Decade_2 (2004-2013)

Average Sediment Yield
(tons/ha/decade)



(c)Decade_3 (2014-2023)

Average Sediment Yield
(tons/ha/decade)

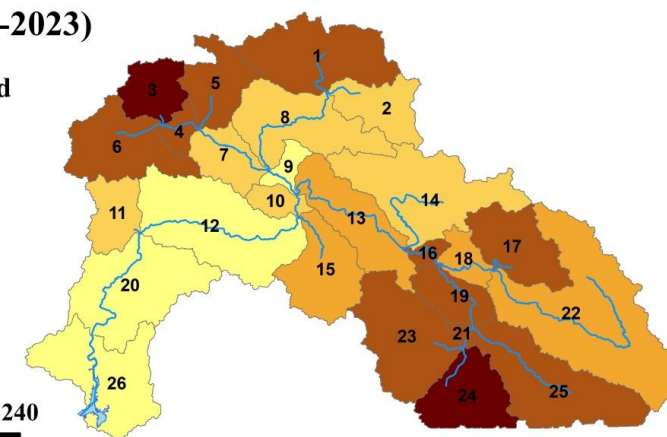
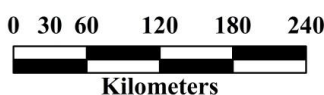
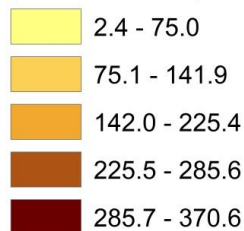


Figure 4. Average sediment yield spatial trend over three decades.

Figure 4 illustrate that the sediment yield in subbasins has been changing in the past three decades due to the land use and Land cover changes (LULC), type of soil, and steepness of the land.

5.2.1. Decade_1 (1994-2003)

The first decade (1994-2003) was characterized by high sediment yield in Subbasin 3 with values ranging from 293.9 to 385.3 tons per hectare each decade. The above sediment yield can be attributed to the presence of a large percentage of AGRL and BARR (Arshad,2024) parcels in the study area with moderate to steep slopes and highly erodible I-

B-U-2c soils. These components have very significant contributions on the erosion process and transportation of sediment. The other sub-basins of the region including but not limited to 6, 4, 5, 1, 17, 16, 19, 21, 23, 24, and 25 have also exhibited increased sediment yield rates of between 215.8 to 293.8 tons per hectare each decade. Characteristics of these sub-basins include intensive land use in agriculture, steepness of slopes, high erodibility of soils such as GLACIER and I-B-U-2c leading to increased sediment yields. Sediment yields are moderate in sub-basins 11, 13, 15, 18 and 22 with values at 143.3 to 215.7 tons per hectare per decade. This is because the area under study has features of low and gently sloping lands with less erosion prone soils, hence the availability of both agricultural land and woods(Arshad,2024) . The subbasins 2, 8, 7, 9, 10, and 14 are considered as the low sediment yielding subbasins with the yields varying between 57.3 to 143.3 tons per hectare each decade. The subbasins have a greater area covered by woods and pastures which are capable of producing ground cover (Arshad,2024). Further, the slope of these sub basins is gently inclined with slope gradients ranging from 0-15 percent and the soils of these sub basins are more authoritative and not easily eroded hence reducing the level of sediment yield. Low sediment yields are seen in subbasins 12, 20, and 26, with yields of 5.9 to 57.2 tons per hectare per decade. Such aspects as the presence of large tracts of forest land, gentle slopes of the landscape and soil stability can therefore be associated with this.

5.2.2. Decade_2 (2004-2013)

Decade two map reveals that subbasin 3 had the highest sediment yield with a range of 300.5 to 382.9 tons/ha/decade. The observed phenomenon can be attributed to steady factors including a high level of land use in agriculture, steep slopes, and highly erodible types of soil (Arshad,2024). The subbasins categorized as having high sediment yield, specifically subbasins 6, 4, 5, 1, 17, 16, 19, 21, 23, 24, and 25, continue to retain their elevated levels of sediment production. This is attributed to the continuous land use and slope characteristics in these subbasins, resulting in sediment yields ranging from 222.2 to 300.4 tons per hectare every decade. Subbasins 13, 15, 18, and 22 are still classified as having medium yield, with yields ranging from 145.7 to 222.1 tons per hectare per decade. On the other hand, subbasins 10, 7, 9, 8, 2, 11 and 14 continue to exhibit low sediment yields, ranging from 57.8 to 145.6 tons per hectare per decade.

5.2.3. Decade_3 (2014-2023)

During the period from 2014 to 2023, Subbasin 24 experiences a significant change as it transitions into the category of very high sediment production. The sediment yields in this category range from 285.7 to 370.6 tons per hectare each decade. The rise in erosion can be attributed to the combination of intensified agricultural practices, the presence of steep slopes, and the vulnerability of the soil. Subbasin 3 consistently exhibits a significantly elevated sediment output within a consistent range. Subbasins 6, 4, 5, 1, 17, 16, 19, 21, 23, and 25 are classified as high yield, with sediment outputs ranging from 225.5 to 285.6 tons per hectare per decade. Subbasins 13, 15, 18, and 22 have medium sediment yields, ranging from 142.0 to 225.4 tons per hectare per decade. The low sediment yield category comprises subbasins 11, 7, 10, 8, 2, and 14, with yields ranging from 75.1 to 141.9 tons per hectare per decade. Subbasins 9, 12, 20, and 26 display very low sediment yields, ranging from 2.4 to 75.0 tons per hectare per decade.

5.2.4. Overall trend of sediment yield across the three decades

The sediment yield during the three decades shows a mixture of stability and variability within the subbasins. Some places maintain their sediment yield categories, while others experience significant increases in sediment yield. Subbasin 3 continuously falls within the "very high" sediment yield category, with a range of 293.9 to 385.3 tons per hectare per decade in Decade 1, 300.5 to 382.9 tons per hectare per decade in Decade 2, and 285.7 to 370.6 tons per hectare per decade in Decade 3. The stability observed can be

attributed to enduring variables such as widespread agricultural land utilization, steep inclines, and erodible soils, which consistently result in elevated erosion rates. Additionally, subbasins 6, 4, 5, 1, 17, 16, 19, 21, 23, and 25 constantly maintain significant levels of sediment deposition in all the decades. In Decade 1, the range is between 215.8 and 293.8 tons per hectare per decade. In Decade 2, the range is between 222.2 and 300.4 tons per hectare per decade. In Decade 3, the range is between 225.5 and 285.6 tons per hectare per decade. The consistent nature of these characteristics, such as land use and slope, suggests that they have remained generally stable across time and continue to contribute to sediment yield in these places. Nevertheless, certain subbasins undergo changes in sediment yield classifications. Subbasin 24 experiences a transformation in its productivity levels over time. In Decades 1 and 2, the productivity varies from 215.8 to 293.8 tons per hectare per decade and 222.2 to 300.4 tons per hectare per decade respectively, which can be considered as "high". However, in Decade 3, the productivity level increases significantly, ranging from 285.7 to 370.6 tons per hectare per decade, which can be classified as "very high". This rise indicates alterations in the intensity of land use, such as an increase in agricultural activities or soil degradation, resulting in greater erosion and sediment output. On the other hand, certain subbasins, such as Subbasin 9, transition from being categorized as "low" in Decades 1 and 2, with values ranging from 57.3 to 143.3 tons per hectare per decade and 57.8 to 145.6 tons per hectare per decade, to being classified as "very low" in Decade 3, with a range of 2.4 to 75.0 tons per hectare per decade. This shift may suggest enhancements in land management methods or natural recovery processes that have successfully decreased the amount of silt produced. Subbasins 12, 20, and 26 consistently maintain a "very low" categorization throughout all three decades, with ranges of 5.9 to 57.2 tons/ha/decade in Decade 1, 2.4 to 57.7 tons/ha/decade in Decade 2, and 2.4 to 75.0 tons/ha/decade in Decade 3. The consistent nature of these places implies that they have upheld steady land use patterns, advantageous slope conditions, and resilient soils that effectively avoid substantial erosion and sediment movement.

Subbasin sediment yields range from 2.4 to 75.0 tons/ha/decade in Decade 3 to 385.3 tons/ha/decade in Decade 1. Most of this heterogeneity is caused by land use intensity, slope steepness, and soil erodibility in various subbasins. Slope, land usage, and erosion-prone soils increase sediment outputs. Sheltering land cover, low slopes, and stable soils restrict sub-basin sediment transfer. This fluctuation is due to land usage, slope, and erodibility. Thus, soil and erosion, agricultural growth, and deforestation in certain sub-basins may boost sediment supply. Better land use or afforestation may have prevented silt buildup. Higher land use intensity and more sensitive soils on steeper slopes cause greater erosion and sediment in subbasins. Thus, soil structure and organic matter restrict erosion (Brady & Weil, 2016). High human activity and steep slopes may cause landslides, which deposit silt. Land use and slope changes have not affected certain subbasins, while others have major sediment production fluctuations due to land management or natural factors. High sediment production needs special conservation efforts, whereas low quantities indicate excellent land management. Our present study is to identify land use, soil, and slope variables that regulate subbasin sediment production.

6. Discussion

The calibration and validation results show that the SWAT model has successfully and well simulated the hydrological processes in the Upper Indus Basin. The mean flow rate observed during the calibration period was 2426.66 cubic meters per second which is slightly lower than the overestimated predicted mean flow of (2855.13 cms). This overestimation is in line with other empirical research conducted in similar geographical areas. In a study by Tantelinaiina et al. (2021), the similar study showed that the SWAT model

tends to overestimate the values. This could be explained by the fact that the model is sensitive to some parameters particularly in areas with intricate hydrological cycles.

The R^2 value of 0.89 and NSE of 0.84 showed that the observed and simulated data were closely related and thus gave the model a “Very good” rating. Sharma et al. (2020) found a similar trend in the Brahmaputra River Basin where SWAT model relatively had strong agreement with the observed flow data but overestimated the actual flow.

The obtained value of the PBIAS -17.7% during calibration is within the acceptable limit of 20% hence supporting the positive result of “Very good”. The RSR value of (0.39) also supports the model robustness as it shows that the errors are indeed very small compared to the variation in the data. The indicators are in agreement with those outlined by Tanteliniaina et al. (2021) in their assessment of the SWAT model in Madagascar, found similar efficiencies.

During the validation period, the model consistently overestimated the mean flow by generating a value of 2890.02 cms while the actual observed mean flow was 2447.44 cms. Nevertheless, the model remained remarkably accurate as depicted by the R^2 of 0.81, NSE of 0.68, and PBIAS of -18.1%, which are all within the acceptable range. Also, Zhang et al. (2022) have shown that the SWAT model has been proven to be reliable in the mountainous areas, capturing most of the observed data within the credible range though with a large prediction uncertainty as indicated by the p-factor and r-factor values of 0.69 and 0.71 respectively.

The significant impact of precipitation to the river system is shown by the precipitation/streamflow ratio of 0.78, which shows that 78% of the precipitation within the watershed affects streamflow. This observation aligns with the findings of Zhang et al. (2023), who documented a comparable proportion in the Yangtze River Basin, where seasonal rainfall has a substantial influence on the flow of water. An analysis of the Baseflow/Total Flow ratio of 0.39 indicates that groundwater accounts for 39% of the whole streamflow, a critical factor in sustaining flow during dry seasons. Gupta et al. (2022) reported comparable results in the Ganges Basin, where baseflow played a significant role in streamflow, especially during periods when the monsoon season is not there. The ratio of 0.61 between Surface Runoff and Total Flow indicates that the bulk of streamflow originates from surface runoff, a pattern that has been likewise seen in Pereira et al. (2021) for the Amazon Basin. A ratio of 0.16 for Percolation/Precipitation underscores the substantial contribution of percolation to groundwater recharge, which aligns with the findings of Singh and Jain (2020) on the Indian subcontinent. Nevertheless, the Deep Recharge/Precipitation is restricted to 0.01, suggesting a poor level of deep groundwater replenishment, which is a prevalent situation in several watersheds, as noted by Wang et al. (2021) in the Loess Plateau. Indeed, the ET/Precipitation ratio of 0.05 highlights the significance of evapotranspiration in the process of water being returned to the atmosphere, which is consistent with the conclusions drawn by Martinez et al. (2022) in Mediterranean vegetation.

During the monsoon season in Northern Pakistan, the watershed experiences an average of 505.35 mm of surface runoff per year. This runoff is essential for carrying materials from upland areas into streams and rivers, especially during periods of vigorous rainfall. These results align with the observations made by Ahmed et al. (2021), who noted comparable patterns of runoff in mountainous regions of the Himalayas. The monsoon rains are an essential aspect of surface runoff as well as sediment transport in the subsequent layers of these areas. The upland sediment yields in the watershed, which range from a high of (5,772.90 Mg/ha) to an average of 2,086.09 Mg/ha point to the fact that there is a lot of sediment loss from the terrain. Consistent with the findings of Khan and Ali (2022) who investigated the erosion processes in the Hindu Kush region, it can be expected that slope gradient, soil type, land use, and vegetation cover may affect the rate of sediment yield. The substantial maximum sediment yield indicates that specific regions

within the watershed, maybe those affected by deforestation or inadequately controlled agricultural areas, make a disproportionate contribution to sediment depletion. Chaudhry et al. (2020) found similar results, with their study showing that Northern Pakistan's deforested regions produce large amounts of sediment. There is a net loss of sediment in the stream channel with a value of (-2,082.52 Mg/ha), which implies that rivers and streams are stores rather than sources of sediment. Rahman et al. (2021) conducted a study that showed that stream in the same topographical area tend to store more sediment than they transport, which makes them to act as sediment sinks.

The trends identified in terms of sediment yield in the sub-basins of Upper Indus Basin over the past three decades are in agreement with the outcomes of previous SWAT model studies conducted in the same region. The analysis done in this study suggests that Subbasin (3) had a very high ability to produce large quantities of sediment, consistent with the study by Bao et al. (2017). This study showed that subbasins with similar topographic properties including steep slopes, large glacier areas, and high land use for agriculture have persistently experienced increased sediment yields due to their vulnerability to erosion.

This study reveals that subbasins (6, 4, 5, 1, 17, 16, 19, 21, 23, and 25) have high levels of sediment production. These findings are consistent with Dowlatabadi and Zomorodian (2016) which utilize SWAT and MODFLOW models also reveals that sediment yields are high in areas with steep slopes and intense land use that supports the findings of this study.

The marked increase in sediment production in Subbasin (24) from a high level to a very high level over the third decade points towards the increased human activities in the form of agriculture. This pattern has also been observed in other related research works. The differences identified suggest adaptation to alterations in land use, a pattern also seen in other works like Liu et al. (2020) that analyzed the growth of sediment generation connected with the expansion of agriculture in glaciated basins. However, Ateeq-Ur-Rehman et al. (2018) has also established these phenomena while assessing the broader patterns of land use changes in the Upper Indus Basin with a specific focus on agricultural growth. From the results of their research, the authors concluded that these changes have led to an increase in sediment yield because of accelerated erosion.

On the other hand, subbasins 12, 20, and 26 revealed minimal levels of sediment yield throughout the whole course of the study. As evidenced by Hallouz et al. (2017), subbasins with similar land cover, including dense forests, and gentle slopes are associated with low sediment yield over a longer time. Applying the proper land management techniques in these areas is expected to yield positive outcomes as far as minimizing erosion is concerned. This is in accordance with previous research that has employed the SWAT model in comparable geographical areas (Keshtegar et al., 2023).

The scientific literature provides ample evidence of the great range of sediment yields observed in the subbasins, from very low (2.4 to 75.0 tons per ha per decade) to very high (up to 385.3 tons per ha per decade). The size of the range is therefore influenced by the interaction of land use, slope and soil erodibility, which are all known to play a vital role in erosion and sediment transport processes (Liu et al., 2020; Shendge et al., 2018).

7. Conclusion

For sensitivity analysis, calibration, and validation, SWAT-CUP interfaced with sequential uncertainty fitting (SUFI-2). Four performance metrics— R^2 , NSE, RSR, and PBIAS—measured model efficiency. Sensitivity study employed 22 model parameters. SWAT-Cup demonstrated excellent performance throughout the 1994-2008 calibration period, with R^2 of 0.89, NSE of 0.84, PBIAS of -17.7%, and RSR of 0.39, indicating a strong correlation between observed and simulated flows. The model performed well during

validation (2009-2023), with $R^2 = 0.81$, $NSE = 0.68$, $PBIAS = -18.1\%$, and $RSR = 0.57$. Calibration and validation for the upper indus basin (UIB) watershed at Besham Qila gauge station show robust and accurate model simulations. The water balance ratios demonstrate that streamflow receives 78% of precipitation, surface runoff 61%, baseflow 39%, percolation 16%, deep recharge 1%, and evapotranspiration 5%. Sediment dynamics reveal an annual average surface runoff of 505.35 mm, upland sediment outputs of 5,772.90 to 2,086.09 Mg/ha, and an instream sediment change of -2,082.52 Mg/ha, demonstrating significant sediment deposition in stream channels that increases flood risk. Decadal sediment production drops over 30 years. In the first decade, yield was 5.9–385.3 tons/ha/decade. This range declined to 2.4 to 382.9 tons/ha/decade in the second decade and 2.7 to 370.6 in the third.

8. Recommendations

The Tarbela Reservoir watershed needs reforestation, terracing, and check dams in high-yield subbasins to reduce sedimentation. Continuous sediment and hydrological monitoring, sustainable land use, and soil conservation education will improve adaptive management measures. Advocating for conservation regulations and encouraging stakeholder participation can help control sediment and maintain reservoir storage capacity and hydropower efficiency. The sediment inflow data from the Tarbela Dam covered only September and October averages, while SWAT outputs reflected annual sediment generation, limiting direct comparisons. ERA-5 climate data, though comprehensive, showed variations from real-time sediment data. Ground-measured climate data, though costly, would improve accuracy and is recommended for future studies.

Funding: This paper is a part of an HEC funded mobility research grant PERIDOT's work.

Conflicts of Interest: The authors declare no conflicts of interest.

References

- Abebe, Z. D., & Sewnet, M. A. (2014). Adoption of soil conservation practices in North Achefer district, Northwest Ethiopia. *Chinese Journal of Population Resources Environment* 12(3), 261-268.
- Ahl, R. S., Woods, S. W., & Zuuring, H. R. (2008). Hydrologic Calibration and Validation of SWAT in a Snow-Dominated Rocky Mountain Watershed, Montana, U.S.A. *JAWRA Journal of the American Water Resources Association*, 44(6), 1411-1430. doi:https://doi.org/10.1111/j.1752-1688.2008.00233.x
- Ahmed, S., Khan, S., & Mahmood, S. (2021). Hydrological responses of the Himalayan region to monsoon rainfall: A SWAT model approach. *Journal of Mountain Science*, 18(4), 945-958. https://doi.org/10.1007/s11629-020-6367-4
- Annandale, G. W., Morris, G. L., & Karki, P. J. (2016). Extending the life of reservoirs: sustainable sediment management for dams and run-of-river hydropower.
- Aslam, M. S. (1992). Pakistan Space and Upper Atmosphere Research Commission. Science Technology Agency, Space Activities in the Asia Pacific Region 53-55.
- Ateeq-Ur-Rehman, M., Bui, D. T., & Rutschmann, P. (2018). Wavelet neural networks and automated model calibration to predict reservoir sedimentation. *Journal of Hydrology*, 560, 453-467.
- Ayele, G. T., Kuriqi, A., Jemberrie, M. A., Saia, S. M., Seka, A. M., Teshale, E. Z., . . . Jeong, J. (2021). Sediment yield and reservoir sedimentation in highly dynamic watersheds: the case of Koga Reservoir, Ethiopia. *Water* 13(23), 3374.
- Bao, A., Wang, Y., & Meng, F. (2017). Hydrological modeling of the Upper Indus Basin: A case study from a high-altitude glacierized catchment, Hunza. *Water*, 9(1), 17. https://doi.org/10.3390/w9010017
- Brady, N. C., & Weil, R. R. (2016). The nature and properties of soils (15th ed.). Pearson.
- Britannica, E. (2020). Reservoir. from In *Encyclopædia Britannica* https://www.britannica.com/technology/reservoir
- Chaudhry, M. R., Nadeem, M. A., & Qasim, M. (2020). The impact of deforestation on sediment yield in Northern Pakistan: An assessment using SWAT. *Environmental Monitoring and Assessment*, 192(5), 304. https://doi.org/10.1007/s10661-020-8258-9

12. Dowlatabadi, S., & Zomorodian, S. M. A. (2016). Conjunctive simulation of surface water and groundwater using SWAT and MODFLOW in the Firoozabad watershed. *KSCE Journal of Civil Engineering*, 20(1), 485-496. <https://doi.org/10.1007/s12205-015-0302-1>
13. Foteh, M. I., Ahmed, S. I., Yimam, Y. T., Birhanu, B. S., & Tadesse, M. G. (2018). Assessment of soil erosion hazard in the Beressa watershed, Blue Nile basin, Ethiopia, using the SWAT model. *Environmental Monitoring and Assessment*, 190(6), 1-12.
14. Gashaw, T., Tulu, T., Argaw, M., & Tadesse, T. (2022). Impact of land use/land cover changes on soil erosion and sediment yield in the Rib watershed, Ethiopia. *Environmental Challenges*, 9, 100577. <https://doi.org/10.1016/j.envc.2022.100577>
15. Gaupp, F., Hall, J., & Dadson, S. (2015). The role of storage capacity in coping with intra-and inter-annual water variability in large river basins. *Environmental Research Letters*10(12), 125001.
16. Goel, M., & Jain, S. K. (1996). Evaluation of reservoir sedimentation using multi-temporal IRS-1A LISS II data. *Asian-Pacific remote sensing GIS journal*8(2), 39-43.
17. Goel, M., Jain, S. K., & Agarwal, P. (2002). Assessment of sediment deposition rate in Bargi Reservoir using digital image processing. *Hydrological sciences journal*47(S1), S81-S92.
18. Gupta, R., Tiwari, M. K., & Singh, V. (2022). Groundwater contribution to streamflow in the Ganges Basin during non-monsoon seasons. *Hydrological Processes*, 36(4), e14578. <https://doi.org/10.1002/hyp.14578>
19. Hallouz, F., Meddi, M., Mahé, G., Alirahmani, S., & Keddar, A. (2017). Modeling of discharge and sediment transport through the SWAT model in the basin of Harraza (Northwest of Algeria). *Water Science*, 64(1), 1-10. <https://doi.org/10.1016/j.wsj.2017.12.004>
20. Houquin, C. (2010). The relationship between large reservoirs and seismicity. *Water Power Dam Construction*
21. ICOLD. (2020). World Register of Dams: General Synthesis. 2020. Retrieved from https://www.icold-cigb.org/GB/world_register/general_synthesis.asp
22. Ijam, A., & Al-Mahamid, M. (2012). Predicting sedimentation at Mujib dam reservoir in Jordan. *Jordan Journal of Civil Engineering*, 6(4), 448-463.
23. Jorgensen, S. E., Loffler, H., Rast, W., & Straskraba, M. (2005). *Lake and reservoir management*: Elsevier.
24. Kellner, E. (2021). The controversial debate on the role of water reservoirs in reducing water scarcity. *Wiley Interdisciplinary Reviews: Water*8(3), e1514.
25. Keshtegar, B., Piri, J., Hussan, W. U., Ikram, K., Yaseen, M., Kisi, O., Adnan, R. M., Adnan, M., & Waseem, M. (2023). Prediction of sediment yields using a data-driven radial M5 tree model. *Water*, 15(1437), 1-28. <https://doi.org/10.3390/w15071437>
26. Khan, Z. H., & Ali, Z. (2022). Erosion processes and sediment yields in the Hindu Kush region: A case study from Northern Pakistan. *Catena*, 207, 105718. <https://doi.org/10.1016/j.catena.2021.105718>
27. Lal, R. (2001). Soil degradation by erosion. *Land Degradation & Development*, 12(6), 519-539. <https://doi.org/10.1002/ldr.472>
28. Lindström, A., & Grani, J. (2012). Large-scale water storage in the water, energy and food nexus: Perspectives on benefits, risks and best practices: Stockholm International Water Institute.
29. Liu, W., Zhang, M., Zhang, J., & Song, Y. (2020). Preliminary research and application of the MIKE SHE model in Jialingjiang river basin. *IOP Conference Series: Earth and Environmental Science*, 304(2). <https://doi.org/10.1088/1755-1315/304/2/022029>
30. Malik, M. A., Dar, A. Q., & Jain, M. K. (2022). Modelling streamflow using the SWAT model and multi-site calibration utilizing SUFI-2 of SWAT-CUP model for high altitude catchments, NW Himalaya's. *Modeling Earth Systems and Environment*, 8(1), 1203-1213. [doi:10.1007/s40808-021-01145-0](https://doi.org/10.1007/s40808-021-01145-0)
31. Martinez, L., Gomez, J., & Ramirez, A. (2022). Evapotranspiration patterns in Mediterranean ecosystems under changing climate conditions. *Journal of Hydrology*, 608, 127691. <https://doi.org/10.1016/j.jhydrol.2022.127691>
32. Mazhar, N., Mirza, A. I., Abbas, S., Akram, M. A. N., Ali, M., & Javid, K. (2021). Effects of climatic factors on the sedimentation trends of Tarbela Reservoir, Pakistan. *SN Applied Sciences*3, 1-9.
33. Merina, R. N., Sashikkumar, M., Rizvana, N., & Adlin, R. (2016). Sedimentation study in a reservoir using remote sensing technique. *Applied ecology environmental research*14(4), 296-304.
34. Moiseev, I. (2000). Experience with Designing and Building Earth-Fill Dams. *Hydrotechnical Construction*34(8-9), 412-414.
35. Mukherjee, S., Veer, V., Tyagi, S. K., & Sharma, V. (2007). Sedimentation Study of Hirakud Reservoir through Remote Sensing Techniques. *Journal of Spatial Hydrology*7(1).
36. Nayab, A., & Faisal, M. (2018). Water Management in Tarbela Dam By using Bayesian Stochastic Dynamic Programming in Extreme Inflow Season. *Journal of Civil Environmental Engineering*8(02).
37. Arshad, N. (2024). Simulation of sediment yield and deposition trends using SWAT model: A case study of Tarbela Dam (Master's thesis, Lahore College for Women University, Lahore, Pakistan).

38. Paudel, P., Shrestha, S., Babel, M. S., & Shrestha, N. K. (2021). Application of SWAT model to assess the climate change impacts on water balance and hydrological extremes in a transboundary river basin of Nepal. *Environmental Earth Sciences*, 80(15), 1-19. <https://doi.org/10.1007/s12665-021-09854-8>
39. Pereira, M., Souza, R., & Oliveira, A. (2021). Surface runoff and streamflow in the Amazon Basin: A SWAT model analysis. *Water Resources Research*, 57(6), e2020WR028976. <https://doi.org/10.1029/2020WR028976>
40. Perera, D., Williams, S., & Smakhtin, V. (2023). Present and Future Losses of Storage in Large Reservoirs Due to Sedimentation: A Country-Wise Global Assessment. 15(1), 219.
41. Pradhanang, S. M., Anandhi, A., Mukundan, R., Zion, M. S., Pierson, D. C., Schneiderman, E. M., . . . Frei, A. (2011). Application of SWAT model to assess snowpack development and streamflow in the Cannonsville watershed, New York, USA. *Hydrological Processes*, 25(21), 3268-3277. doi:<https://doi.org/10.1002/hyp.8171>
42. Rahman, K., Maringanti, C., Beniston, M., Widmer, F., Abbaspour, K., & Lehmann, A. (2013). Streamflow Modeling in a Highly Managed Mountainous Glacier Watershed Using SWAT: The Upper Rhone River Watershed Case in Switzerland. *Water Resources Management*, 27(2), 323-339. doi:10.1007/s11269-012-0188-9
43. Rahman, N., Hussain, Z., & Ali, F. (2021). Simulation of sedimentation patterns in Tarbela Dam using MIKE 21C model. *Journal of Water Resources Planning and Management*, 147(6), 04021045.
44. Roca, M. (2012). Tarbela Dam in Pakistan. Case study of reservoir sedimentation.
45. Sharma, A., Goyal, M. K., & Sarma, A. K. (2020). Application of the SWAT model for climate change impact assessment on water resources in a sub-basin of Brahmaputra River, India. *Journal of Water and Climate Change*, 11(3), 905-923. <https://doi.org/10.2166/wcc.2020.029>
46. Shendge, R. B., Chockalingam, M. P., Saritha, B., & Ambica, A. (2018). SWAT modeling for sediment yield: A case study of Ujjani reservoir in Maharashtra, India. *International Journal of Civil Engineering and Technology*, 9(1), 245-252.
47. Silvio, G., & Hotchkiss, R. (1995). Two Years Activity of ICCORES (International Coordinating Committee on Reservoir Sedimentation). Paper presented at the Sixth International Symposium on River Sedimentation.
48. Singh, S., & Jain, M. (2020). Groundwater recharge and percolation in the Indian subcontinent: A regional study. *Water Science and Technology*, 82(10), 1983-1994. <https://doi.org/10.2166/wst.2020.338>
49. Tamene, L., Park, S., Dikau, R., & Vlek, P. (2006). Analysis of factors determining sediment yield variability in the highlands of northern Ethiopia. *Geomorphology* 76(1-2), 76-91.
50. Tanteliniaina, M., Rahaman, M. H., & Zhai, J. (2021). Assessment of the Future Impact of Climate Change on the Hydrology of the Mangoky River, Madagascar Using ANN and SWAT. *Water*, 13. doi:10.3390/w13091239
51. UCSUSA. (2013). The Sources of Energy. Retrieved from http://www.ucsusa.org/clean_energy/our-energy-choices/the-sources-of-energy.html
52. Vemu, S., & Udayabhaskar, P. (2010). An integrated approach for prioritization of reservoir catchment using remote sensing and geographic information system techniques. *Geocarto international* 25(2), 149-168.
53. Wang, X., Li, Y., & Zhang, Y. (2021). Deep groundwater recharge estimation in arid regions of the Loess Plateau using the SWAT model. *Journal of Hydrology*, 594, 125973. <https://doi.org/10.1016/j.jhydrol.2020.125973>
54. Wang, X., Shao, X., & Li, D. (2003). Sediment deposition pattern and flow conditions in the Three Gorges Reservoir: A physical model study. *Tsinghua Science Technology* 8(6), 708-712.
55. WWF. (2013). Dam facts and figures. Retrieved from http://wwf.panda.org/what_we_do/footprint/water/dams_initiative/quick_facts/
56. Zhang, L., Wang, H., & Huang, C. (2023). Water balance analysis in the Yangtze River Basin using the SWAT model. *Hydrology and Earth System Sciences*, 27(2), 879-893. <https://doi.org/10.5194/hess-27-879-2023>
57. Zhang, Y., Li, H., & Huang, C. (2022). Evaluation of SWAT model performance for simulating hydrological processes in mountainous regions. *Hydrology Research*, 53(3), 674-688. <https://doi.org/10.2166/nh.2022.022>